Unravelling molecular mechanisms in the fluorescence spectra of doxorubicin in aqueous solution by femtosecond fluorescence spectroscopy

P. Changenet-Barret, T. Gustavsson, D. Markovitsi, I. Manet, S. Monti

▶ **To cite this version:**

P. Changenet-Barret, T. Gustavsson, D. Markovitsi, I. Manet, S. Monti. Unravelling molecular mechanisms in the fluorescence spectra of doxorubicin in aqueous solution by femtosecond fluorescence spectroscopy. Physical Chemistry Chemical Physics, 2013, 15 (8), pp.2937-2944. 10.1039/C2CP44056C . hal-00807306

HAL Id: hal-00807306
https://hal.science/hal-00807306

Submitted on 3 Apr 2013

HAL is a multi-disciplinary open access archive for the deposit and dissemination of scientific research documents, whether they are published or not. The documents may come from teaching and research institutions in France or abroad, or from public or private research centers.

L'archive ouverte pluridisciplinaire **HAL**, est destinée au dépôt et à la diffusion de documents scientifiques de niveau recherche, publiés ou non, émanant des établissements d'enseignement et de recherche français ou étrangers, des laboratoires publics ou privés.

Journal Name

Dynamic Article Links►

Cite this: DOI: 10.1039/c0xx00000x

www.rsc.org/xxxxxx

ARTICLE TYPE

Unravelling molecular mechanisms in the fluorescence spectra of Doxorubicin in aqueous solution by femtosecond fluorescence spectroscopy

Pascale Changenet-Barret,*[a] Thomas Gustavsson,[a] Dimitra Markovitsi,[a] Ilse Manet,*[b] and Sandra Monti[b]

Received (in XXX, XXX) XthXXXXXXXXX 20XX, Accepted Xth XXXXXXXXX 20XX
DOI: 10.1039/b000000x

Doxorubicin (DOX) is a potent anti-tumoral agentwidely used for cancer therapy. Despite numerous studies,the fluorescence properties of DOX, usually exploited for the characterization ofthe interaction with biological media,have until now led to controversial interpretations, mainly due to self-association of the drug in aqueous solution. We present here thefirst femtosecond study of DOX based on measurements with fluorescence up-conversion technique in combination with time-correlated single photon counting using the same laser source. We provide evidence that fluorescence signals of DOX stem from monomers and dimers. DOX dimerization induces a dramatic decrease in the fluorescence quantum yield from 3.9×10^{-2} to 10^{-5}associated to the red shift of the fluorescence spectrum by *ca* ~25 nm.While the fluorescence lifetime of themonomer is 1 ns, the dimer fluorescence is found to decay with a lifetime of about 2 ps.In contrast to monomers, the fluorescence anisotropy of dimers is found to be negative. These experimental observations are consistent with an ultrafastinternal conversion (<200 fs) between two exciton states, possibly followed by a charge separation process.

1. Introduction

Anthracycline antibiotics are very efficient anti-tumoral agents extensively employed in chemotherapy for the treatment of a large variety of cancers. Although the exact mechanism of their action is still not clear, theyare thought to act as inhibitors of both DNA replication and RNA transcription. It is generally accepted that this biological activity relies on their interactions with B-DNA structures,[1-3] through the intercalation of the anthraquinone moiety at the GC sequences, while the drug sugar moiety interacts with the minor DNA groove.[4, 5]Doxorubicin (DOX), also known as Adriamycin (Fig. 1), is a natural anthracyclinecompound which is considered to be a prototypical anti-tumordrug.[6-9]DOX consists of a tetrahydroxy-anthraquinonechromophore with a pendant glycosyl moiety, representing the essential structural features of anthracyclines. The anthraquinonechromophore contains two hydroxyl groups respectively positioned in direct neighbourhood of the central oxo group.

Owing to its great efficacy, DOX is still widely used in clinical practice, in spite of the deleterious side effects mainly related to its cardiotoxicity. More recently, another serious problem in DOX treatment has emerged connected to the development of some resistant cancer cell lines.[6, 7]In the frame of its clinical use, the poor solubilityof DOX in aqueous solution is considered to be a serious drawback, affectingboth its transport across the cell membranes and its biological activity.[10]In this respect, the development of nano-sized drug carriersfor DOX has recently attracted a lot of research interest, since it may offer the right solutions to overcome the problems related to cytotoxicity, solubility and resistance.[11-19]

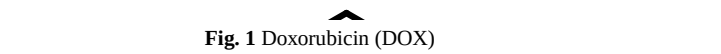

Fig. 1 Doxorubicin (DOX)

In view of the design of innovative biomedical applications involving DOX, understanding the nature of the interactions of DOX with its environment,once dissolved in aqueous solution,is of paramount importance. In this respect, the physical properties of DOX in aqueous solution have been the object of a large variety of studies including UV-vis absorption, NMR, circular dichroism (CD) and fluorescence spectroscopy.[20-28] While concentration dependent absorption, NMR and CD spectra are generally interpreted in terms ofdimer formation, there is only a limited and controversialunderstanding of the intrinsic fluorescence properties of the drug in solution. Aggregation is

known to induce a significant decrease of the fluorescence quantum yield attributed to the formation of non-fluorescent dimers.[23, 27] Fluorescence of DOX in aqueous solution has been reported alternatively to exhibit monoexponential or biexponential decays.[24, 28-33]The origin of such bi-exponentialdecays is not fully clarified and has led to various interpretations. The presence of two ground-state tautomers or two ground-state conformers differing in their inter-molecular hydrogen bonds with the solvent, as well as the formation of astrongly fluorescent photodegradation producthave been proposed.[24, 32-35]These contrasting interpretations prompted us to examine the intrinsic photophysics of DOXin aqueous solution prior to studying the interaction of the drug with biological species or nano-sized particles. The aimofthis work is to disentanglethe various molecular contributions to the fluorescence signals taking also into consideration the aggregation tendency of DOX. To this purpose, a combination of femto- and picosecond fluorescence techniques was used. The fluorescence decays, fluorescence anisotropy decays at selected wavelengths and time-resolved spectra have been measured for different concentrations of DOX,in aqueous solutions, at physiological conditions. The overall results are discussed in the frame of the literature on anthracyclines and their close derivatives.

2. Materials and Methods

2.1. Materials

DOX (purity >95%)was purchased from ALEXIS Biochemicals and used without any further purification. Solutions of DOX were prepared in ultra-pure water delivered by a Millipore MilliQ system. Aqueous solutions of DOX at physiological conditions were prepared in 10 mM Tris buffer, at pH 7.4, with 1 mM EDTA and 50 mM NaCl. For the time resolved-fluorescence measurements, concentration of DOX was varied between 10 μM and1 mM.

2.2. Steady-statespectroscopy

Steady-state absorption and fluorescence spectra were recorded with a double-beam UV-visible spectrophotometer (Perkin-Elmer Lambda 900) and spectrofluorimeter (SPEX Fluorolog-3). For steady-state fluorescence measurements, 1 cm thickness quartz cells were used. The fluorescence spectra were corrected for the wavelength-dependent response of the instrument.

2.3. Time-resolved fluorescence measurements

Time-resolved fluorescence measurements were carried out with two different techniques: time-correlated single photon counting (TCSPC) and fluorescence up-conversion (FU) described in detail elsewhere.[36, 37]In both cases, the laser source was a mode-locked Ti-sapphire laser providing 120-fs pulses at 800 nm with a repetition rate of 76 MHz (MIRA, Coherent). For excitation, frequency-doubled pulses at 400 nm were used.For the TCSPC measurements, the laser repetition rate was reduced to 4.75 MHz using a pulse-picker (Coherent) and the average excitation power was set to less than 1 mW. The polarization of the exciting beam was controlled with a zero-order half-wave plate. For the FU measurements, the average excitation power was set to 60 mW. The fluorescence from the sample was collected with parabolic mirrors and mixed with the residual fundamental in a 0.5 mm type I BBO crystal to generate the sum-frequency light. The latter was spectrally filtered in a monochromator and detected by a photomultiplier in single-photon counting mode. The spectral resolution was approximately5 nm. Time-resolved fluorescence spectra in the 500-700 nm region were recorded at magic angle, by spectral scans on three different time scale, with time steps of 100 fs, 1 ps and 10 ps respectively. The acquisition procedure of these spectra has been addressed in details in a previous report.[38] Note that the different spectral components of the up-converted signal travel at different speeds through the various optics due to the group velocity dispersion. Therefore,the delay stage was adjusted in order to compensate the wavelength-dependent difference in group velocity, during the spectral scans. The time-integrated spectra were corrected *a posteriori*for the spectral response of the detection, with regards to the steady-state fluorescence spectrum.

Both for TCSPC and FU, fluorescence decays were measured with parallel and perpendicular excitation-detection polarization configurations by adjusting the polarization of the excitation beam with a zero-order half-wave plate.

All time-resolved fluorescence measurements were performed at room temperature (20 ± 1°C), under aerated conditions. For TCSPC, the sample solution was placed in a 1 cm thick quartz cell and magnetically stirred.For FU, 1 mm or 2 mm thick quartz cells were used. The cell was kept rotating during acquisitions. Absorption and fluorescence spectra of the sample were checked before and after experiment.

2.4. Data analysis

Total fluorescence kinetics F(t) were constructed from $I_{par}(t)+2\times G\times I_{perp}(t)$, fluorescence anisotropy decays r(t) were calculated according to $(I_{par}(t) - G\times I_{perp}(t)) / F(t)$. G is the ratio of the sensitivity of the detection system to parallel (vertical) and perpendicularly (vertical) polarized excitation light. In our case G was measured to be 1.0 for both fluorescence set-up.

Total fluorescence kinetics were independently fitted with a sum of exponential functions, convoluted by a Gaussian function representing the instrument response function. The full width at half maximum (FWHM) of the Gaussian was found to be about 280 ± 15 fs at all probed wavelengths.

The rotational diffusion time τ_{Rot} and the fluorescence anisotropy $r_0$were extracted from the global fit of $I_{par}(t)$ and $I_{perp}(t)$ with convolution fitting routines, following equations:

$$I_{par}(t)=\left(1+2*r(t)\right)*f(t)$$

$$I_{perp}=(1-r(t))*f(t)$$

$$\text{with} r(t)=\sum_{i=1}^{m} r_i \exp(-t/\tau_{i\,Rot}),$$

$$\text{and} f(t)=\sum_{j=1}^{n} a_j * \exp\left(-t/\tau_j\right).$$

The full set of kinetic profiles extracted from the time-resolved fluorescence spectra were globally fitted, after dimensional reduction and noise filtering by singular value decomposition (SVD),[39] as previously described.[40] The results of the global analysis are presented as Decay Associated Spectra (DAS) corresponding to the spectral distribution of the amplitudes associated to the time components.

This journal is © The Royal Society of Chemistry [year]

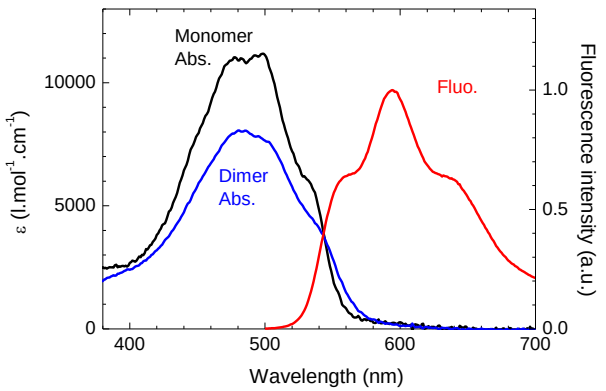

Fig. 2 Black and blue lines are the absorption coefficients of DOX monomers and one DOX molecule in dimers, respectively, calculated assuming a dimerization binding model in the analysis of a series of spectra obtained for varying DOX concentration.[28]In red, corrected steady-state fluorescence spectra (λ_{exc} = 350, 400 or 450 nm) for 10 μM DOX solution in Tris buffer.

3. Results and discussion

3.1. Steady-state spectroscopy of DOX and self-association

Fig. 2 illustrates the steady-state absorption and fluorescence spectra of a 10 μM DOX solution in Tris buffer at pH 7.4. These spectra display similar features to those of 1,4-dihydroxy anthraquinone (quinizarin) in protic solvents.[41]The absorption spectrum of DOX displays one main band centred at 490 nm associated to the $^1A \rightarrow {}^1L_b$ π,π* transition polarized along the long axis[42] anda shoulder around 360 nm attributed to partially forbidden n,π* transitions involving the three C=O groups.[22]

The fluorescence spectrum of DOX exhibits three distinct peaks around 560, 594 and 638 nm associated to a vibrational progression with a frequency lying in the range of 1,000-1,200 cm^{-1}.[21] As in the case of quinizarin, the vibrational structures observed in the absorption and the fluorescence spectra stem fromthe symmetric modes associated with the C=O bending, skeletal stretching and OH bending motions of the dihydroxyanthraquinone moiety.[21, 43]

The visible region of the absorption spectrum of DOX is known to be strongly influenced by the protonation state of the dihydroxyanthraquinone moiety whereasit is barely sensitive to the protonation state of the sugar part which is not conjugated to the central aromatic ring. The pK_a of the daunosamine-NH_3^+ group and one of the phenolic OH groups of the anthracyclinering B in aqueous solutionsbeing 8.15 and 10.16, respectively.[44, 45] Under physiological conditions, the phenol moietyremains thereforeneutral whereas the daunosamin-NH_3^+ is expected to be positively charged for a large fraction of molecules (~82%).[22, 42]

Aggregation is also known to affect significantly the absorption spectrum of DOX leading to a slight broadening of the main absorption band with a significant hypochromism in the spectral region between 415 nm and 540 nm and a weak hyperchromism in the spectral region above 540 nm.[20, 46]Literature provides quite different values for the association constant of DOX in aqueous solutions, depending on the experimental conditions.[20-22, 26-28] For concentrations below5 mM, a simple dimerization model is in general considered sufficient to describe theself-association process.[27]Under these conditions, a previous analysis of the absorption spectra of DOX in Tris buffer, at physiological pH yielded a dimerization constant with log(K_d) = 4.8±0.1.[28]Using this value, it can be estimated that, a fraction of 47% of the drug undergoesdimerization in a 10 μM DOX solution.

The existence of dimers with two distinct geometries has been suggested by Agrawal *et al*. on the basis of the 2D NOESY NMR spectra of DOX in D_2O and Molecular Dynamics (MD) calculations.[27] In these two conformations, the arrangement of the two DOX units would consist of the stacking of the aglycone moieties either in parallel or anti-parallel orientations, with the methoxy substituent of D ring pointing toward the exterior or the interior of the interplanar space, respectively.[27]In the frame of the exciton theory, formation of such aggregates leads in principle to a blue shift of the absorption spectrum with regards to that of the monomeric units.[47]The important hypochromism at the absorption maximum and the concomitant hyperchromism in the low energy part of the absorption spectrum of dimerscould be explained by asignificant deviation from acollinear arrangement of the transition dipole moments of the two DOX units. Indeed,MD calculations predicted significant angles between the two aromatic planes in the parallel and the antiparallel conformations,respectively.[27]Additional indication forexcitonic couplingin DOX dimers has been found in the CD absorption spectra of the drug, at concentrationsabove 10^{-5} M.[28]Theyexhibit a characteristic excitonic bisignate doublet in the 420-580 nm region, from which a ~3000 cm^{-1}Davydov splitting can be estimated.

The fluorescence quantum yield of 10 mM DOX solution for excitation at 480 nm is known to be 3.9×10^{-2}.[28, 33]Until now, DOX dimershave been considered as "non-fluorescent" species whose presencenoticeably reducesthe fluorescence intensity of the drug solutionwithout altering the shape of the fluorescence spectrum.[27]Such a behavior provides evidence that the steady-state fluorescence spectrum of DOX arises mainly from the monomers. At this point, it is noteworthy that, in contrast to the recent study of Rana *et al*.,[33] no effect of the excitation wavelength on the steady-state fluorescence spectrum of DOX in Tris buffer, can be observed. This, *a priori*, discards a possible contribution of various ground-state species to the fluorescence signals.

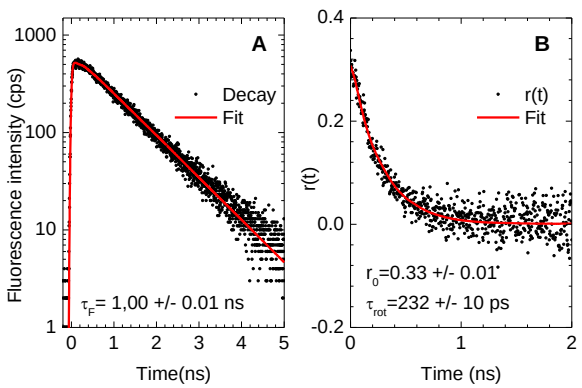

Fig. 3(**A**) Typical total fluorescence decay and (**B**)fluorescence anisotropy decay of 10 μM DOX in Tris buffer, at 650 nm. The red solid

lines correspond to fits with mono-exponential functions convoluted with IRF. The fit of the anisotropy was extracted from a global fit of $I_{par}(t)$ and $I_{perp}(t)$.

3.2. Nanosecond fluorescence decays and concentration effects

A typical total fluorescence decay of a 10 μM DOX solution measured by TCSPC at 650 nm is shown in Fig. 3. DOX fluorescence exhibits a mono-exponential decay with a lifetime of 1 ns, independently of the emission wavelength. There is only weak variation of the fluorescence decays with the drug concentration. Slightly faster fluorescence decay (0.93 ns *vs* 1 ns) has been found in a 450 μM DOX solution, in which 88% of the drug molecules undergo dimerization.Theselifetimes arein good agreement with recent TCSPC measurements.[28, 32]The exponential behaviour of DOX however markedly differs from some previous TCSPC measurements reporting biexponential fluorescence decays.[24, 29-33]Recently, the observation of biexponential decays has been correlated to the formation of some photodegradation products depending on the excitation wavelength and intensity.[32] In our case, the mono-exponential fluorescence decay of DOX in Tris buffer shows that, under our excitation conditions, the formation of photodegradation products can be excluded. It also precludes the above-mentioned contribution of several long-lived ground-state tautomers or conformers to the fluorescence signals.

As illustrated in Fig. 3.B, the fluorescence anisotropy of a 10 μM DOX solutionexhibits a fast exponential decay with a time constant of 232±10 ps with $r_0 = 0.33\pm0.02$. A similar decay has also been observed for a higher concentration (450 μM) of DOX. Using the Debye-Stokes-Einstein relationship, the rotational diffusion time is given by $\tau_{rot} = \eta V/k_B T$, where V, T and η are the hydrodynamic volume of DOX, the temperature and the viscosity of the solvent, respectively. With η = 1 cP, we estimate the effective volume of DOX to 938 $Å^3$. This value is fully consistent with the volume of the anthracycline moiety.[48]Since the same anisotropy decay is observedfor the concentrated solution of DOX, it provides strong evidence that, in the nanosecond regime, the fluorescence comes from the monomers solely.

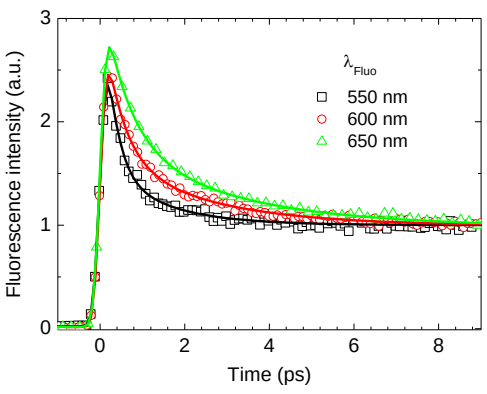

Fig. 4 Total fluorescence decays of 380 μM DOX in Tris buffer,at 550, 600 and 650 nm. The fits with a three-exponential function convoluted with a Gaussian representing the instrumental response function (FWHM 280 fs) are shown by solid lines.

3.3. Ultrafast fluorescence decays: concentration effects

In the femto-picosecond regime, the fluorescence of DOX in Tris buffer exhibits a more complex behavior. Kinetic traces recorded by FU at three wavelengths are represented in Fig. 4. Individual FU kinetic profiles were fitted using a three-exponential function where the longest characteristic time was fixed to 1 ns, in accordance with the fluorescence lifetime obtained from TCSPC. Results of the fits are gathered in Table 1.

Table 1. Time constants and amplitudes obtained from the individual fits of the fluorescence decays measured for 380 μM DOX in Tris buffer.

DOX / Tris *c = 380 μM*	a_1 τ_1	a_2 τ_2	a_3 τ_3
550 nm	0.55±0.03 271±20 fs	0.17±0.01 1.4±0.2 ps	0.28±0.01 1ns
600 nm	0.45±0.02 440±35 fs	0.23±0.02 2.2±0.1 ps	0.32±0.01 1ns
650 nm	0.43±0.02 607±46 fs	0.27±0.02 2.8±0.1 ps	0.30±0.01 1ns

Decays were fitted using a tree-exponential function where the longest time was fixed to 1 ns.

As seen in Table 1, at all probed wavelengths, the fluorescence decays exhibits two fast components of a few hundred femtoseconds and about 2 ps respectively, followed bythe nanosecond component. The relative amplitudes (a_1 and a_2) of the two fast time components exhibit a clear wavelength dependence concomitant with a significant increase of τ_1 and τ_2 with wavelength. The amplitudes of thesetwo fast components decrease dramatically with the drug concentration. In order to illustrate this effect, the normalized fluorescence decays measured at 600 nm for DOX solutions at four different concentrations are represented in Fig. 5. The result of the individual fits of the fluorescence decay traces measured at 600 nm is given in Table 2. For the highest concentrations, two time-constants, one sub-ps and one ranging between 1-3 ps, are needed to reproduce the fast part of the FU fluorescence decays, whereas for the lowest concentration (38 μM), only one picosecond time constant suffices.This provides evidence that the two fast components of the fluorescence decays of DOX are correlated with the dimers.

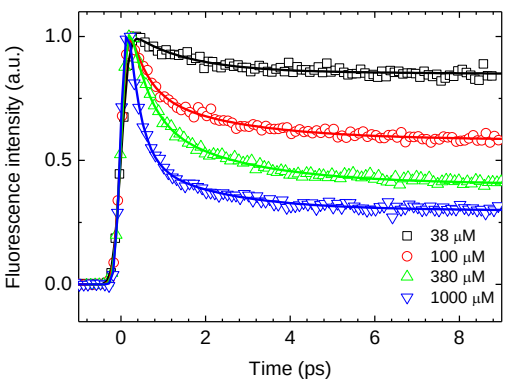

Fig. 5 Typical total fluorescence decays of DOX in Tris buffer, at 600 nm for different concentrations of the drug. The fit with a three-exponential

This journal is © The Royal Society of Chemistry [year]

function convoluted with a Gaussian representing the instrumental response function (FWHM 280 fs) are represented by the solid lines.

Table 2. Time constants and amplitudes obtained from the individual fits of the fluorescence decays measured for DOX in Tris buffer, at four different concentrations.

DOX / Tris λ_{Fluo} = *600 nm*	a_1 τ_1	a_2 τ_2	a_3 τ_3
800 µM 9% mon.	0.50±0.02 455±20 fs	0.29±0.02 2.1±0.1 ps	0.21±0.01 1ns
380 µM 13% mon.	0.45±0.02 441±35 fs	0.23±0.01 2.2±0.1 ps	0.32±0.01 1ns
100 µM 23% mon.	0.35±0.10 256±107 fs	0.24±0.03 1.9±0.3 ps	0.41±0.01 1ns
38 µM 35% mon.	- -	0.18±0.01 1.3±0.1 ps	0.82±0.01 1ns

Decays were fitted using a tree-exponential function where the longest time was fixed to 1 ns. The fraction of monomers for each concentration of the drug is given in the first column.

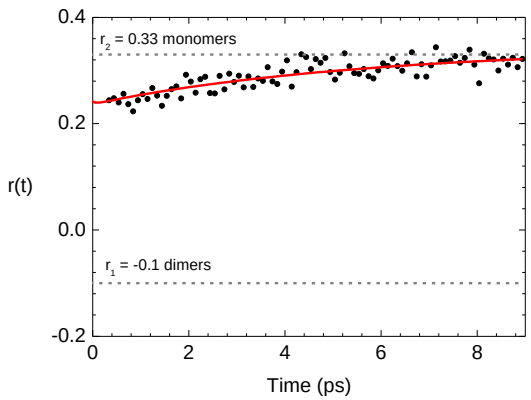

Fig. 6 Typical fluorescence anisotropy decay of 800 µM DOX, at 600 nm.The fit of the anisotropy represented by the red solid line has been extracted from the global fit of $I_{par}(t)$ and $I_{perp}(t)$.The dashed gray lines indicate the values of the anisotropy extracted from the fit (r_1= -0.10 ± 0.02 and r_2= 0.33 ± 0.02).

Fig. 6 displays the typicalfluorescence anisotropy signal recorded on a time scale of 10 ps, at all the probed wavelengths. As shown in Fig. 6, the anisotropy traces exhibit a *ca.* 6 ps rise. This peculiar behaviour could be explained by the superposition of fluorescence stemming from two different species, namely the dimers and the monomers. The short-lived fluorescence of the dimers is associated witha negative anisotropy (r_1 = -0.10 ± 0.02), whereas the long-lived fluorescence of the monomers is associated with a positive anisotropy (r_2 = 0.33 ± 0.02), as observed in the TCSPC measurements. This positive anisotropy remains constant over the whole observed time interval.

The fluorescence anisotropy depends on the natures of the absorbing and emitting species (states). The negative value of the dimer anisotropy indicates an important electronic relaxation, on a time scale much faster than our time resolution (<200 fs). In other terms, the electronic transition associated with the dimer fluorescence is different from that associated to the photon absorption.The fluorescence anisotropy is given by:

$$r(0)=\frac{1}{5}(3\cos^2(\theta)-1)$$

whereθ is the angle between the two transition dipoles. Theanisotropy of -0.1 correspond toan angle of 66°.Conversely, the high anisotropy of the monomer fluorescence shows that,in this case, the excitation directly populates the emitting state.

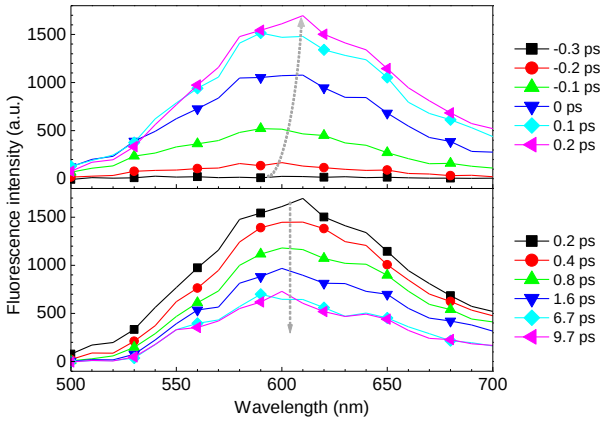

Fig. 7 Time-resolved fluorescence spectra of 380 µM DOX in Tris buffer between –0.3 and 0.2 ps (upper panel) andbetween 0.2 and 9.7 ps (lower panel).

3.4. Origin of the ultrafast biexponential fluorescence decays of DOX dimers

The short excited-state lifetime of the dimer fluorescence indicates the existence of non-radiative processes that are not present in the monomers. The origin of the biexponential nature of the dimer fluorescence decays deserves further discussion. As shown in Table 1, the slight increase of the two short lifetimes with increasing wavelength suggests a dynamical red shift of the fluorescence spectra of DOX on the femto-picosecond time scale. In order to confirm this hypothesis, the whole time-resolved spectra of DOX in Tris bufferat two different concentrationswere recorded. Fig. 7 illustrates the time evolutionof the spectra, over a time scale of 10 ps, at a DOX concentration of 380 µM. It can be seen that the fluorescence spectrumof DOX exhibits a fast dynamical shift to the red within the duration of the apparatus function. Beyond a time delay of 0.2 ps, the fluorescence spectrum of DOX starts to decrease in intensity. After 6 ps, the fluorescence spectrum remains constant over the probed time window.

The global kinetic analysis of the time-resolved fluorescence spectra of DOXrequired the sum of three exponential components. Fig. 8 displays the corresponding DAS.Their associated lifetimes are 0.22 ± 0.02 ps, 1.54 ± 0.05 ps for the 380 µM DOX solution and 0.14 ± 0.01 ps, 1.45 ± 0.06 ps for the 100 µM DOX solution, respectively. The longer time component associated to the monomer fluorescence has been fixed to 1 ns, like for the individual fits. It is worth noting that this global analysis procedure, which implies a compartmental description of the spectro-temporal evolution of the system, is not well-adapted if the fluorescence spectra display continuous time-dependent spectral shifts, which is the case in the present work. Still, thisprocedure is judged to provide a satisfactory qualitative description of the time-dependentfluorescence spectrum of

DOX.Consequently, the global procedure can provide time constants thatdiffer slightly from those obtained by individual fits performed at given wavelengths.

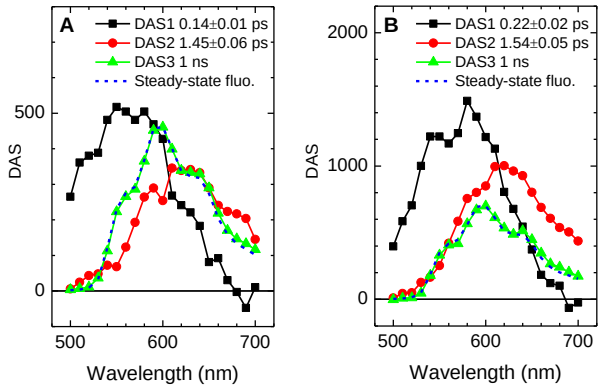

Fig. 8 Decay-associated spectra DAS (solid lines) of the three time components found in the SVD analysis of the time-resolved fluorescence spectra of DOX in Tris buffer, at two different concentrations: (**A**)100 μM and(**B**) 380 μM.For comparison, the steady-state fluorescence spectrum of DOX is repesented by the blue short-dashed lines.

As illustrated on Fig. 8, the relative amplitudes of the two first DAS with respect to DAS3 are clearly correlated to the drug concentration. Both of them can therefore be ascribed to the spectro-temporal changes of the dimer fluorescence spectrum. DAS1 (0.14 and 0.22 ps, respectively) displays the characteristic features of a fast dynamicalStokes shift of the fluorescence spectrum of dimers causing the continuous red shift of the band. The positive contribution between 500 nm and 650 nm in DAS1 arises from the fast initial decay on the blue side of thefluorescence band whereas the positive contribution above 650 nm corresponds to the rise on the red side of the fluorescence band. DAS2 (~1.5 ps) and DAS3 (1 ns)illustrate the fluorescence decay of the dimers and the monomers, respectively.The fluorescence spectrum ofthe dimers (DAS2) issignificantly red-shifted with regards to that of the monomers(DAS3).At this point, it is worth noting that the percentage of photons emitted by the dimers ($a_2\tau_2/\sum_{i=2}^{3} a_i\,\tau_i$, see Table 1) corresponds toless than 0.2% of the total fluorescence. The fluorescence quantum yield of the dimers is estimated to$\approx 10^{-5}$.

The fast dynamical Stokes shift of the dimer fluorescence in Tris buffercan be described by an exponential function with a time component of 0.24 ± 0.05 ps (see SI Figure S1).Such a shiftcan be attributed to different processes occurring on the femto-picosecond time scale. First, a rationale may be offered by solvation dynamics, which is known to produce a spectrum like DAS1 with a negative amplitude in the red wing.For comparison, solvation dynamics of water has been shown to involve three components (<1 ps), with an average time of about 0.5 ps.[49-51] The dynamical shift of the DOX fluorescence, which is mostly described by DAS1 (~0.2 ps), appears to be twice faster than the average time of the solvation dynamics of water. This could be explained by the short lifetime of dimers preventing the observation of the entire solvation process. Besides the solvation dynamics, vibrational relaxation may also contribute to the earliest dynamics of the dimer fluorescence (DAS1). Such a process would lead to a rapid narrowing of the emission band, in particular on the blue side, in agreement with the large amplitude decays observed around 550 nm (see Table 1).

The fluorescence spectrum of DOX dimers represented by DAS2 is found to be 25-nm red-shiftedwith respect to that of the monomers. From the fraction of absorbing dimers *vs.*monomers, it can be estimated that the transition moment associated with the dimer fluorescence is about 5 times smaller than that of the monomer. The concomitant depolarization of the dimer fluorescence, observed immediately after excitation,is consistent withthe excitationof anupper exciton statefollowed by a fast internal conversionto a lowerexciton statefrom whichemission arises. For this reason, the electronic transitions related to photon absorption and photon emission have different polarization.Note that the fast conversion between the two exciton states can also be associated to important vibrational relaxation in the lower state, in line with the above-mentioned fast decay of the blue side of the dimer fluorescence.

Due to the weakertransition moment of the dimer fluorescence, one would expect its fluorescence lifetime to be longer than that of the monomer.In contrast, the acceleration of the dimer fluorescence decay with respect to that of the monomer indicates the presence of additional non-radiative relaxation pathways.For instance, such fast excited-state decays have been reported inrhodamine 800 dimers.[52]They were attributed to the dissociation of the dimers in their excited-state leading to the formation of excited monomers.[52]Such a process is not consistent with our experimental observationssincenodelayed rise of the monomers fluorescence is observed.Alternately, fast fluorescence decay in bichromophoric molecules such as perylene diimide[53] and naphthalene diimides[54] have been assigned to a charge separationbetween the two units. In this context, we tentatively assign the fast fluorescence decay of DOXdimers to a charge separation process,occurringon a time scale of 1-2 ps,which is comparable to the diffusive part of the solvation dynamics. In agreement with this attribution, the lifetime of DOX dimers in D_2O is found to beslightly longer to that observed in Tris bufferand pure H_2O (see SI Figures S2 and S3 andTables S1 and S2). Even though literature data on D_2O solvation dynamics are scarce, the average solvation times of D_2O islonger than that of H_2O.[50, 51]

4. Conclusion

In this report, we have presented the first fluorescence study of DOX using a combination of time-resolved techniques with a time resolution up to 200 fs, in order to disentangle the various molecular contributions to the fluorescence of the drug. Fluorescence decays of DOX in aqueous solution, at physiological conditions, were found to exhibit three exponential components whose amplitudes display a strong dependence on the drug concentration. The fluorescence lifetimes span from 0.2 ps to 1 ns. The fast components in the femto-picosecond regime can be unambiguously ascribed to the fluorescence of DOX dimers whereas the slowest component is due to the monomers.

In contrast to some previous time-resolved fluorescence studies of DOX by TCSPC, we did not find any evidence of contributions of different tautomeric forms or photodegradation

This journal is © The Royal Society of Chemistry [year]

products.[24, 32-35] The global analysis of the time-resolved fluorescence spectra of DOX, measured at two different concentrationsin the femto-picosecond regime, allowed the extraction of the fluorescence spectra associated to monomers and dimers. The fluorescence spectrum of monomers is similar to the steady-state fluorescence spectrum of DOX and has a lifetime of 1 ns. In contrast, dimers display a significantly red-shifted and structureless fluorescence spectrum which undergoes a fast dynamic Stokes shift during a few hundred femtoseconds before vanishing in about 2 ps.

The time-resolved fluorescence anisotropy decays provide evidence that the two species contribute to the fluorescence signals with distinct anisotropies, respectively. Dimer fluorescence is associated with a negative anisotropy of -0.1 while anisotropy of monomer fluorescence is equal to 0.33. Such observation is consistent with the occurrence of a fast internal conversion between two excitonic states followed by a charge separation process leading to the fast decay of the dimer fluorescence. Comparative measurements in salt-rich aqueous solution, pure water and heavy water suggest that this latter process could bepromoted bythe solvation dynamics.

Acknowledgements

The research leading to these results has received funding from COST MP0802 and from LASERLAB-EUROPE (grant agreement no. 228334, EC's Seventh Framework Programme).

Notes and references

[a]*Laboratoire Francis Perrin, CEA/DSM/IRAMIS/SPAM – CNRS URA 2453, 91191 Gif-sur-Yvette, France. Fax: + 33 169 088 707; Tel: +33 169 081 940; E-mail: pascale.changenet-barret@cea.fr*

[b]*Istituto per la SintesiOrganica e la Fotoreattività, CNR, via P. Gobetti 101, 40129 Bologna, Italy. Fax: +39 051 639 9844; Tel: +30 051 639 9808; E-mail: ilse.manet@isof.cnr.it*

† Electronic Supplementary Information (ESI) available: (i) Typical total fluorescence decay of DOX (800 μM) in D_2O, (ii) Time constants and amplitudes obtained from the individual fits of the fluorescence decays of DOX in D_2O, (iii) Typical total fluorescence decay of DOX (800 μM) in H_2O,(iv) Time constants and amplitudes obtained from the individual fits of the fluorescence decays of DOX in H_2O.See DOI: 10.1039/b000000x/

References

1. D. Dal Ben, M. Palumbo, G. Zagotto, G. Capranico and S. Moro, *Curr. Pharm. Des.*, 2007, **13**, 2766-2780.
2. S. Moro, G. L. Beretta, D. D. Ben, J. Nitiss, M. Palumbo and G. Capranico, *Biochem.*, 2004, **43**, 7503-7513.
3. G. Capranico, F. Zunino, K. Kohn and Y. Pommier, *Biochem.*, 1990, **29**, 562-569.
4. C. Temperini, L. Messori, P. Orioli, C. D. Bugno, F. Animati and G. Ughetto, *Nucleic Acids Res.*, 2003, **31**, 1464-1469.
5. C. Frederick, L. Williams, G. Ughetto, G. Vandermarel, J. Vanboom, A. Rich and A. Wang, *Biochem.*, 1990, **29**, 2538-2549.
6. A. Thorburn and A. E. Frankel, *Mol. Cancer Ther.*, 2006, **5**, 197-199.
7. G. Minotti, P. Menna, E. Salvatorelli, G. Cairo and L. Gianni, *Pharmacol. Rev.*, 2004, **56**, 185-229.
8. G. L. Beretta and F. Zunino, in *Anthracycline Chemistry and Biology II: Mode of Action, Clinical Aspects and New Drugs*, ed. Springler-Verlag, Berlin2008, pp. 1-19.
9. F. Arcamone, F. Animati, G. Capranico, P. Lombardi, S. Pratesi, S. Manzini, R. Supino and F. Zunino, *Pharmacol. Ther.*, 1997, **76**, 117-124.
10. M. Dalmark and H. H. Storm, *J. Gen. Physiol.*, 1981, **78**, 349-364.
11. B. Cerroni, E. Chiessi, S. Margheritelli, L. Oddo and G. Paradossi, *Biomacromolecules*, 2011, **12**, 593-601.
12. P. Horcajada, T. Chalati, C. Serre, B. Gillet, C. Sebrie, T. Baati, J. F. Eubank, D. Heurtaux, P. Clayette, C. Kreuz, J. S. Chang, Y. K. Hwang, V. Marsaud, P. N. Bories, L. Cynober, S. Gil, G. Ferey, P. Couvreur and R. Gref, *Nat. Mater.*, 2010, **9**, 172-178.
13. H. Huang, Q. Yuan, J. S. Shah and R. D. K. Misra, *Adv. Drug Deliv. Rev.*, 2011, **63**, 1332-1339.
14. C. T. Huynh, M. K. Nguyen, J. H. Kim, S. W. Kang and B. S. Kim, *Soft Matter*, 2011, **7**, 4974-4982.
15. A. Lowery, H. Onishko, D. E. Hallahan and Z. Z. Han, *J. Controlled Release*, 2011, **150**, 117-124.
16. D. M. Ren, F. Kratz and S. W. Wang, *Small*, 2011, **7**, 1051-1060.
17. F. Wang, Y. C. Wang, S. Dou, M. H. Xiong, T. M. Sun and J. Wang, *ACS Nano*, 2011, **5**, 3679-3692.
18. Y. Yan, A. P. R. Johnston, S. J. Dodds, M. M. J. Kamphuis, C. Ferguson, R. G. Parton, E. C. Nice, J. K. Heath and F. Caruso, *ACS Nano*, 2010, **4**, 2928-2936.
19. R. Anand, F. Manoli, I. Manet, S. Daoud-Mahammed, V. Agostoni, R. Gref and S. Monti, *Photochem. Photobiol. Sci.*, 2012, **11**, 1285-1292.
20. M. Menozzi, L. Valentini, E. Vannini and F. Arcamone, *J. Pharm. Sci.*, 1984, **73**, 766-770.
21. L. Angeloni, G. Smulevich and M. P. Marzocchi, *Spectrochim. Acta, Pt. A: Mol. Spectrosc.*, 1982, **38**, 213-217.
22. L. Gallois, M. Fiallo and A. Garnier-Suillerot, *Biochim. Biophys. Acta*, 1998, **1370**, 31.
23. K. K. Karukstis, E. H. Z. Thompson, J. A. Whiles and R. J. Rosenfeld, *Biophys. Chem.*, 1998, **73**, 249-263.
24. T. Htun, *J. Fluores.*, 2004, **14**, 217-222.
25. M. P. Evstigneev, V. V. Khomich and D. B. Davies, *Russ. J. Phys. Chem.*, 2006, **80**, 741-746.
26. I. J. McLennan, R. E. Lenkinski and Y. Yanuka, *Can. J. Chem.*, 1985, **63**, 1233-1238.
27. P. Agrawal, S. K. Barthwal and R. Barthwal, *Eur. J. Med. Chem.*, 2009, **44**, 1437-1451.
28. R. Anand, S. Ottani, F. Manoli, I. Manet and S. Monti, *RSC Adv.*, 2012, **2**, 2346-2357.
29. N. Husain, R. A. Agaria and I. M. Warner, *J. Phys. Chem. A*, 1993, **97**, 10857-10861.
30. R. Goldman, T. Facchinetti, D. Bach, A. Raz and M. Shinitzky, *Biochim. Biophys. Acta*, 1978, **512**, 254-269.
31. T. G. Burke, M. Israel, R. Seshadri and J. H. Doroshow, *Biochim. Biophys. Acta*, 1989, **982**, 123-130.
32. K. Nawara, P. Krysinski and G. J. Blanchard, *J. Phys. Chem. A*, 2012, **116**, 4330-4337.
33. D. K. Rana, S. Dhar, A. Sarkar and S. C. Bhattacharya, *J. Phys. Chem. A*, 2011, **115**, 9169-9179.
34. M. Fiallo, A. Laigle, M. N. Borrel and A. Garnier-Suillerot, *Biochem.*, 1993, **45**, 659-665.
35. O. Hovorka, V. Subr, D. Vetvicka, L. Kovar, J. Strohalm, M. Strohalm, A. Benda, M. Hf, K. Ulbrich and B. Rihova, *Eur. J. Pharm. Biopharm.*, 2012, **76**, 514-524.
36. T. Gustavsson, A. Sharonov and D. Markovitsi, *Chem. Phys. Lett.*, 2002, **351**, 195.
37. D. Markovitsi, D. Onidas, F. Talbot, S. Marguet, T. Gustavsson and E. Lazzarotto, *J. Photochem. Photobiol. A: Chem.*, 2006, **183**, 1-8.
38. T. Gustavsson, G. Baldacchino, J.-C. Mialocq and S. Pommeret, *Chem. Phys. Lett.*, 1995, **236**, 587-594.
39. E. R. Henry and J. Hofrichter, *Methods Enzymol.*, 1992, **210**, 129.
40. P. Changenet-Barret, P. Plaza, M. M. Martin, H. Chosrowjan, S. Taniguchi, N. Mataga, Y. Imamoto and M. Kataoka, *J. Phys. Chem. C*, 2009, **113**, 11605-11613.
41. D. K. Palit, H. Pal, T. Mukkherjee and J. Mittal, *J. Chem. Soc. Farad. Trans.*, 1990, **86**, 3861-3869.
42. M. M. L. Fiallo, H. Tayeb, A. Suarato and J. P. S. A. Garnier-Suillerot, 1998, 87, 967-975., *J. Pharm. Sci.*, 1998, **87**, 967-975.
43. G. Smulevich, L. Angeloni, S. Giovannardi and M. P. Marzocchi, *Chem. Phys.*, 1982, **65**, 313-322.
44. R. Kiraly and R. B. Martin, *Inorganica Chimica Acta-Bioinorganic Chemistry*, 1982, **67**, 13-18.

45. L. Messori, C. Temperini, F. Piccioli, F. Animati, C. D. Bugno and P. Orioli, *Biorg. Med. Chem.*, 2001, **9**, 1815-1825.
46. J. B. Chaires, N. Dattagupta and D. M. Crothers, *Biochem.*, 1982, **21**, 3927-3932.
47. M. Kasha, H. R. Rawls and M. Ashraf El-Bayoumi, *Pure Appl. Chem.*, 1965, **11**, 371-392.
48. J. P. Rasimas and G. J. Blanchard, *J. Phys. Chem.*, 1995, **99** 11333-11338.
49. R. Jimenez, G. R. Fleming, P. V. Kumar and M. Maroncelli, *Nature*, 1994, **369**, 471-473.
50. D. Pant and N. E. Levinger, *J. Phys. Chem.*, 1999, **103**, 7846-7852.
51. M. Sajadi, M. Weinberger, H.-A. Wagenknecht and N. P. Ernsting, *Phys. Chem. Chem. Phys.*, 2011, **13**, 17768–17774.
52. K. Sekiguchi, S. Yamaguchi and T. Tahara, *J. Phys. Chem. A*, 2006, **110**, 2601-2606.
53. J. M. Giaimo, A. V. Gusev and M. R. Wasielewski, *J. Am. Chem. Soc.*, 2002, **124**, 8530-8531.
54. N. Banerji, A. Fürstenberg, S. Bhosale, A. L. Sisson, N. Sakai, S. Matile and E. Vauthey, *J. Phys. Chem. B*, 2008, **112**, 8912-8922.

This journal is © The Royal Society of Chemistry [year]